



UNIVERSITÀ
DEGLI STUDI
FIRENZE

DISEI

DIPARTIMENTO DI SCIENZE
PER L'ECONOMIA E L'IMPRESA

WORKING PAPERS
QUANTITATIVE METHODS FOR SOCIAL SCIENCES

The price-leverage covariation as a measure of the
response of the leverage effect to price and
volatility changes

GIACOMO TOSCANO

WORKING PAPER N. 03/2021

*DISEI, Università degli Studi di Firenze
Via delle Pandette 9, 50127 Firenze (Italia) www.disei.unifi.it*

*The findings, interpretations, and conclusions expressed in the working paper series
are those of the authors alone. They do not represent the view of Dipartimento di
Scienze per l'Economia e l'Impresa*

The price-leverage covariation as a measure of the response of the leverage effect to price and volatility changes

Giacomo Toscano, University of Florence
(giacomo.toscano@unifi.it)

June 18, 2021

Abstract

We study the sensitivity of the leverage effect to changes of the price and the volatility, showing the existence of an analytical link between the latter and the price-leverage covariation under the Constant Elasticity of Variance model. From the financial standpoint, this result allows for the interpretation of the price-leverage covariation as a gauge of the responsiveness of the leverage effect to price and volatility changes. The study of S&P500 high-frequency prices over the period March, 2018-April, 2018, carried out by means of non-parametric Fourier estimators, suggests that empirical data may support this interpretation of the role of the price-leverage covariation.

JEL codes: C14, C58

Keywords: leverage effect, Fourier analysis, price-leverage covariation

1 Introduction

Empirical evidence collected in the literature suggests that the leverage effect, i.e., the (usually negative) correlation between the price and the volatility of a financial asset, is time-varying. For instance, Kalnina and Xiu (2017) point out that the intensity of the leverage effect gets stronger in turbulent periods, that is, in correspondence of volatility spikes or large returns, while Bandi and Renò (2012) model the leverage process as a function of the stochastic volatility of the asset, based on empirical evidence. Thus, in order to get insight into the time-varying dynamics of the leverage process, it may be interesting to study its sensitivity to increments of the volatility or the price.

This can be done analytically in the case of the Constant Elasticity of Variance (CEV) model by Beckers (1980). The CEV model is possibly the most popular example in the class of level-dependent models, that is, models that treat the volatility

process as a deterministic function of the price process. Level-dependent models represent a parsimonious and analytically-tractable tool to reproduce some stylized facts of financial markets, e.g., the implied volatility smile (see, e.g., Derman and Kani (1994); Dupire (1994); Hobson and Rogers (1998)). More recently, a level-dependent model driven by a Fractional Brownian motion has also been introduced, with the aim of reproducing the empirically-observed long-memory property of the volatility (see Araneda (2020)). Specifically, the CEV model is explicitly designed to capture leverage effects. Moreover, under the CEV model, the leverage process can be viewed as a deterministic differentiable function of either the volatility or the log-price, thereby allowing the computation of its analytical derivative with respect to any of these two processes.

In this regard, simple calculations show that both these analytical derivatives depend on the same quantity: the price-leverage covariation. In particular, it emerges that the derivative of the leverage with respect to the price (respectively, the volatility) is equal to the ratio of the price-leverage covariation and the volatility (respectively, the leverage). Additionally, it also emerges that the price-leverage covariation is equal to twice the vol-of-vol process. However, the result related to the analytical derivative of the leverage with respect to the volatility holds more generally. In fact we show that, for this derivative to be equal to the ratio of the price-leverage covariation and the leverage, it is sufficient to assume that the data-generating process is any stochastic volatility model with continuous paths where the vol-of-vol process is a multiple of a power of the variance process. Popular, widely-used examples of stochastic volatility models with this feature, beyond the CEV model, are the model by Heston (1993), the 3/2 model by Platen (1997) and the continuous-time GARCH model by Nelson (1990). Also, in this more general semi-parametric framework, the price-leverage covariation is still a linear function of the vol-of-vol.

The price-leverage covariation has first been studied in Barucci et al. (2003), where the authors derive a model-free indicator of financial instability whose analytical expression depends, other than on the volatility and the leverage, on the price-leverage covariation. However, only recently Sanfelici and Mancino (2020) have provided a consistent non-parametric estimator of the price-leverage covariation, based on the Fourier method by Malliavin and Mancino (2002).

The existence of a theoretical, model-dependent link between the price-leverage covariation and the sensitivity (i.e., the derivative) of the leverage process with respect to the price and the volatility motivates an empirical, model-free investigation of this link. Accordingly, in this paper we conduct this investigation on the sample of S&P500 1-second prices over the period March, 2018 - April, 2018. As a result, we uncover the existence of a statistically-significant linear relationship between the price-leverage covariation scaled by the volatility or the leverage and the cor-

responding numerical derivative of the leverage, computed via finite differences. Remarkably, estimated regressions coefficients are close to 1, thereby suggesting that theoretical predictions provide an accurate proxy of the true derivatives of the leverage for the sample object of study. Note that, to be able to perform this empirical investigation, we have reconstructed the unobservable paths of the volatility, the leverage and the price-leverage covariation from high-frequency prices in a non-parametric fashion through the Fourier methodology (see, respectively, Malliavin and Mancino (2002, 2009); Barucci and Mancino (2010); Sanfelici and Mancino (2020)).

Based on these empirical findings, the price-leverage covariation can be interpreted, from a financial standpoint, as a model-free measure of the responsiveness of the leverage effect to the arrival of new information on the market that causes changes in the price or in the amount of risk perceived by market participants (i.e., in the volatility). Further, additional empirical results suggest that the price-leverage covariation is approximately equal to twice the vol-of-vol for the sample of object of study. Again, this results is line with the prediction of the CEV model, which implies - as already mentioned - that the price-leverage covariation is exactly equal to twice the vol-of-vol. Interpreting the vol-of-vol as the uncertainty about the actual level of risk perceived on the market, this finding suggests that the response of the leverage effect to changes in the price or the volatility is proportional to the intensity of this uncertainty: the larger the latter, the stronger the response of the leverage (and viceversa). Finally, note that the path of the vol-of-vol has also been reconstructed non-parametrically using the Fourier methodology (see Sanfelici et al. (2015)) for this empirical analysis.

The paper is organized as follows. In Section 2 we derive the analytical expressions of the derivatives of the leverage with respect to the price and the volatility under the CEV model. In Section 3 we give a brief description of the non-parametric Fourier estimators of the spot volatility, leverage, vol-of-vol and price-variance covariation and recall their asymptotic properties. Sections 4 and 5 contain, respectively, numerical and empirical results. Finally, Section 6 concludes.

2 Analytical derivatives of the leverage in the CEV framework

Let $X(t)$ denote the price process and assume that its dynamics follow the CEV model, that is,

$$dX(t) = \sigma X(t)^\delta dW(t) + \mu X(t)dt, \quad (1)$$

where W is a Brownian motion on the filtered probability space $(\Omega, \mathcal{F}, (\mathcal{F}_t)_{t \geq 0}, \mathbb{P})$, satisfying the usual conditions, $\mu \in \mathbb{R}$, $\sigma > 0$ and $\delta > 0$. Note that the role of the parameter δ is crucial, as it captures leverage effects. Specifically, if $\delta < 1$, the price and the volatility are negatively correlated, as it commonly happens on equity markets. Instead, if $\delta > 1$, the price and the volatility move in the same direction, according to the so-called inverse leverage effect, a phenomenon usually observed on commodity markets.

Define $x(t) := \ln(X(t))$. Under model (1), the following expressions are obtained for the volatility $v(t)$, the leverage $\eta(t)$, the price-leverage covariation $\chi(t)$ and the vol-of-vol $\xi(t)$:

$$v(t) := \frac{d\langle x, x \rangle_t}{dt} = \sigma^2 e^{2(\delta-1)x(t)}, \quad (2)$$

$$\eta(t) := \frac{d\langle x, v \rangle_t}{dt} = 2(\delta - 1)v(t)^2, \quad (3)$$

$$\chi(t) := \frac{d\langle x, \eta \rangle_t}{dt} = 8(\delta - 1)^2 v(t)^3, \quad (4)$$

$$\xi(t) := \frac{d\langle v, v \rangle_t}{dt} = 4(\delta - 1)^2 v(t)^3. \quad (5)$$

Therefore, the derivatives of the leverage $\eta(t)$ with respect to the log-price $x(t)$ and the volatility $v(t)$ read:

$$\frac{\partial \eta(t)}{\partial x(t)} = \frac{\chi(t)}{v(t)}, \quad (6)$$

$$\frac{\partial \eta(t)}{\partial v(t)} = \frac{\chi(t)}{\eta(t)}. \quad (7)$$

Based on equations (6) and (7), in the CEV framework $\chi(t)$ could be interpreted, from a financial point of view, as the process that captures the response of the leverage to the arrival of new information that causes changes in the volatility and/or the price.

Further, note that the derivative of the leverage with respect to the price in equation (6) is strictly positive, since it is equal to the ratio of two strictly positive processes, $v(t)$ (see (2)) and $\chi(t)$ (see (4)). This implies that on equity markets the leverage effect increases (i.e., the leverage process becomes more negative) in correspondence of a negative return, and viceversa. Instead, the sign of the derivative of the leverage with respect to the volatility in equation (7) depends on the sign of $\eta(t)$. Therefore, if at some point in time $\eta(t)$ is negative, it becomes

more (respectively, less) negative in correspondence of an increment (respectively, reduction) of the volatility. Overall, model-dependent predictions of the sensitivity of the leverage effect to the price and the volatility in equations (6) and (7) are consistent with the empirical findings related to time-varying leverage effects by Kalnina and Xiu (2017) and Bandi and Renò (2012).

Additionally, based on equations (4) and (5), the process $\chi(t)$ is simply equal to twice the vol-of-vol $\xi(t)$ in the CEV framework. From a financial standpoint, this linear link could be interpreted as follows. Taking the volatility as a measure of market risk and the vol-of-vol as a proxy of the uncertainty about the actual level of market risk perceived by market operators, the larger is the latter, the more intense is the response of the leverage to price and market risk changes, as captured by $\chi(t)$.

Remark 1. *For the result in equation (7) to hold and for the price-leverage covariation to be a linear function of the vol-of-vol, it is sufficient to assume that the log-price and the volatility are continuous semimartingales driven by two Brownian motions with constant non-zero correlation parameter and that the diffusion component of the volatility process is a multiple of a power of the volatility process itself. Formally, assume that*

$$\begin{aligned} dx(t) &= \sqrt{v(t)}dW(t) + a(t)dt \\ dv(t) &= \gamma v(t)^\beta dZ(t) + b(t)dt \\ d\langle W, Z \rangle_t &= \rho dt \end{aligned} \tag{8}$$

where: W and Z are Brownian motions on the filtered probability space $(\Omega, \mathcal{F}, (\mathcal{F}_t)_{t \geq 0}, \mathbb{P})$, which satisfies the usual conditions; a , b and v are continuous adapted processes¹; $\rho \in [-1, 1] - \{0\}$, $\gamma \in \mathbb{R}$ and $\beta \in \mathbb{R}$. Then it follows that:

$$\xi(t) = \gamma^2 v(t)^{2\beta}, \tag{9}$$

$$\eta(t) = \rho \sqrt{v(t)} \sqrt{\xi(t)}, \tag{10}$$

$$\chi(t) = \left(\beta + \frac{1}{2}\right) \rho^2 \xi(t). \tag{11}$$

¹The condition $v(t) > 0$ a.s., which is clearly desirable from a financial standpoint, may impose some additional constraints on the parametric form of the drift b (see, e.g., Feller (1951) for the case when b has a mean-reverting structure). However, any additional constraints on the parametric form of b do not interfere with the computations of $\xi(t)$, $\eta(t)$ and $\chi(t)$, as they depend only on the diffusion components of the price and the volatility.

Therefore:

$$\frac{\partial \eta(t)}{\partial v(t)} = \frac{\chi(t)}{\eta(t)}. \quad (12)$$

The semi-parametric specification (8) contains the class of stochastic volatility models where the volatility is a CKLS process (Chan et al. (1992)), such as the Heston model, the continuous-time GARCH model and the 3/2 model. Moreover, it contains also the CEV model, as in (1), which indeed can be rewritten as:

$$\begin{aligned} dx(t) &= \sigma(t)dW(t) + \left(\mu - \frac{1}{2}v(t)\right)dt \\ dv(t) &= \gamma v(t)^\beta dW(t) + \gamma v(t) \left(\mu - \frac{1}{2}(\gamma+1)v(t)\right)dt \end{aligned} \quad (13)$$

where $\gamma = 2(\delta - 1)$ and $\beta = 3/2$.

Assuming the CEV model as the data-generating process, consistent estimators of the derivatives (6) and (7) can be built as the ratio of non-parametric estimators of $\chi(t)$ and, respectively, $v(t)$ or $\eta(t)$. We address this aspect in the next section, using the Fourier methodology.

3 Fourier-based estimation of the analytical derivatives of the leverage in the CEV framework

The Fourier method, introduced by Malliavin and Mancino (2002), is particularly well-suited to build non-parametric estimators of second-order and third-order quantities. As a first step, one obtains estimates of the Fourier coefficients of the latent volatility $v(t)$. Then, the knowledge of these coefficients allows iterating the procedure to compute the Fourier coefficients of the second-order quantities $\xi(t)$ and $\eta(t)$. Finally, a third iteration yields estimates of the coefficients of the third-order quantity $\chi(t)$. In this regard, it is worth noting that these progressive iterations do not involve any differentiation procedure for the pre-estimation of the spot volatility (in order to estimate second-order quantities) or the spot leverage (in order to estimate the third-order quantity $\chi(t)$). Instead, they only require the pre-estimation of integrated quantities, namely the Fourier coefficients. Given the numerical instabilities which are typically linked to differentiation procedures, this feature represents a strength of the Fourier methodology, compared to the realized approach for the estimation of spot processes (see Chapter 8 in Aït-Sahalia and Jacod (2014) for a detailed description of realized spot estimators and their asymptotic properties).

The Fourier estimators of $v(t)$, $\eta(t)$, $\xi(t)$ and $\chi(t)$, which we illustrate in the following, are termed non-parametric in that, for their asymptotic properties to hold, they only require that the processes $x(t)$, $v(t)$ and $\eta(t)$ are continuous semi-martingales. Formally, we assume that:

$$\begin{aligned} dx(t) &= \sqrt{v(t)}dW(t) + a(t)dt \\ dv(t) &= \gamma(t)dZ(t) + b(t)dt \\ d\eta(t) &= \lambda(t)dY(t) + c(t)dt \end{aligned}$$

where W, Z and Y are correlated Brownian motions on the filtered probability space $(\Omega, \mathcal{F}, (\mathcal{F}_t)_{t \geq 0}, \mathbb{P})$, which satisfies the usual conditions, while the processes a, b, c, v, γ and λ are continuous, adapted and bounded in absolute value.

In the following subsections, after briefly illustrating the Fourier estimators of $v(t)$, $\eta(t)$, and $\chi(t)$ and recalling their asymptotic properties, we derive consistent estimators of the derivatives (6) and (7) as the ratio of the Fourier estimators of $\chi(t)$ and, respectively, $v(t)$ or $\eta(t)$. The Fourier estimator of the vol-of-vol $\xi(t)$ is also illustrated, as it will be used in the empirical study of Section 5.

3.1 Fourier estimator of the volatility

Assume that the log-price process $x(t)$ is observable on the grid of mesh size $\rho(n) := 2\pi/n$ over the interval $[0, 2\pi]^2$. Then, for $|k| \leq N$, the k -th (discrete) Fourier coefficient of the volatility is defined as

$$c_k(v_{n,N}) := \frac{2\pi}{2N+1} \sum_{|s| \leq N} c_s(dx_n) c_{k-s}(dx_n), \quad (14)$$

where for any integer $k, |k| \leq 2N$, $c_k(dx_n)$ is the k -th (discrete) Fourier coefficient of the log-return process, namely

$$c_k(dx_n) := \frac{1}{2\pi} \sum_{j=0}^{n-1} e^{-ikt_{j,n}} \delta_j^n(x), \quad (15)$$

where $\delta_j^n(x) := x_{t_{j+1,n}} - x_{t_{j,n}}$, $t_{j,n} = j \frac{2\pi}{n}$, $j = 0, 1, \dots, n$, while the symbol i denotes the imaginary unit, that is, $i = \sqrt{-1}$.

²In applications, we can always assume that the price process $x(t)$ is observed on $[0, 2\pi]$ by re-scaling the actual time interval. Moreover, note that in this Chapter, to simplify the exposition, we assume that the price process is observable on an equally-spaced grid, but, in general, the Fourier method works also with unequally-spaced samples (see Mancino et al. (2017)).

Once the Fourier coefficients of the volatility (14) have been computed, the application of the Fourier-Fejér inversion formula allows reconstructing the volatility path. The definition of the Fourier spot volatility estimator is as follows.

Definition 1. Fourier estimator of the spot volatility

The Fourier estimator of the spot volatility process is defined as the random function of time

$$\widehat{v}_{n,N,S_v}(t) := \sum_{|k| < S_v} \left(1 - \frac{|k|}{S_v}\right) c_k(v_{n,N}) e^{ikt}, \quad (16)$$

where S_v is a positive integer smaller than N , while $c_k(v_{n,N})$ is defined in (14).

The following theorem demonstrates the uniform consistency of the Fourier estimator of the spot volatility (16).

Theorem 1. For any integer $|k| \leq N$, if $N/n \rightarrow 1/2$, the following convergence in probability holds

$$\lim_{n,N \rightarrow \infty} c_k(v_{n,N}) = c_k(v),$$

where $c_k(v)$ is the k -th Fourier coefficient of the volatility process $v(t)$. Moreover, if $N/n \rightarrow 1/2$ and $S_v/n \rightarrow 0$, it holds in probability that

$$\lim_{n,N,S_v \rightarrow \infty} \sup_{t \in (0,2\pi)} |\widehat{v}_{n,N,S_v}(t) - v(t)| = 0.$$

Proof. See Malliavin and Mancino (2009). □

3.2 Fourier estimator of the leverage

As mentioned, the knowledge of the Fourier coefficients of the latent instantaneous volatility $v(t)$ allows treating the latter as an observable process and iterate the procedure for computing the Fourier coefficients in order to reconstruct the leverage process $\eta(t)$. In particular, to estimate the instantaneous leverage $\eta(t)$ we exploit the multivariate version of Fourier method introduced in Malliavin and Mancino (2009). Accordingly, an estimator of the Fourier coefficients of the leverage is given by

$$c_k(\eta_{n,N,M}) := \frac{2\pi}{2M+1} \sum_{|j| \leq M} c_j(dx_n) c_{k-j}(dv_{n,N}), \quad (17)$$

where M is a positive integer smaller than N , $c_j(dx_n)$ is given in (15) and we use the approximation $c_j(dv_{n,N}) \cong ij c_j(v_{n,N})^3$. Then the following theorem holds.

³See, e.g., Chapter 6 in Mancino et al. (2017).

Theorem 2. *If $N/n \rightarrow 1/2$ and $M^2/n \rightarrow 0$ for $n, N, M \rightarrow \infty$, then the following convergence in probability holds*

$$\lim_{n, N, M \rightarrow \infty} c_k(\eta_{n, N, M}) = c_k(\eta),$$

where $c_k(\eta)$ is the k -th Fourier coefficient of the leverage process $\eta(t)$.

Proof. See Barucci and Mancino (2010). □

Finally, a consistent estimator of the instantaneous leverage $\eta(t)$ is obtained as

$$\widehat{\eta}_{n, N, M, S_\eta}(t) := \sum_{|k| < S_\eta} \left(1 - \frac{|k|}{S_\eta}\right) c_k(\eta_{n, N, M}) e^{ikt}, \quad (18)$$

where S_η is a positive integer smaller than M , while $c_k(\eta_{n, N, M})$ is defined in (17).

3.3 Fourier estimator of the vol-of-vol

The knowledge of the coefficients of the volatility process $v(t)$ also allows building an estimator of its quadratic variation, the vol-of-vol $\xi(t)$. In particular, an estimator of the coefficients of $\xi(t)$ is given by

$$c_k(\xi_{n, N, M}) := \frac{2\pi}{2M+1} \sum_{|j| \leq M} c_j(dv_{n, N}) c_{k-j}(dv_{n, N}), \quad (19)$$

where, again, $c_j(dv_{n, N})$ is approximated with $ijc_j(v_{n, N})$. Then the following theorem holds.

Theorem 3. *If $N/n \rightarrow 0$ and $M^4/N \rightarrow 0$ for $n, N, M \rightarrow \infty$, then the following convergence in probability holds*

$$\lim_{n, N, M \rightarrow \infty} c_k(\xi_{n, N, M}) = c_k(\xi),$$

where $c_k(\xi)$ is the k -th Fourier coefficient of the vol-of-vol process $\xi(t)$.

Proof. See Sanfelici et al. (2015). □

Finally, a consistent estimator of the spot vol-of-vol $\xi(t)$ can be obtained as

$$\widehat{\xi}_{n, N, M, S_\xi}(t) := \sum_{|k| < S_\xi} \left(1 - \frac{|k|}{S_\xi}\right) c_k(\xi_{n, N, M}) e^{ikt} \quad (20)$$

where S_ξ is a positive integer smaller than M , while $c_k(\xi_{n, N, M})$ is defined in (19).

3.4 Fourier estimator of the price-leverage covariation

Similarly to what we have done for the volatility process $v(t)$, once its Fourier coefficients have been estimated, we can treat the second-order quantity $\eta(t)$ as an observable process and exploit the multivariate Fourier method to estimate the third-order quantity $\chi(t)$. The following asymptotic result is obtained.

Theorem 4. *If $N/n \rightarrow 1/2$ and $L^2M^2/N \rightarrow 0$ for $n, N, M, L \rightarrow \infty^4$, then the following convergence in probability holds*

$$\lim_{n, N, M, L \rightarrow \infty} c_k(\chi_{n, N, M, L}) = c_k(\chi),$$

where, for L positive integer and smaller than M , we define

$$c_k(\chi_{n, N, M, L}) := \frac{2\pi}{2L+1} \sum_{|j| \leq L} c_j(dx_n) \mathbf{i}^j c_{k-j}(\eta_{n, N, M}).$$

Proof. See Sanfelici and Mancino (2020). □

Accordingly, a consistent spot estimator of the process $\chi(t)$ is defined as

$$\widehat{\chi}_{n, N, M, L, S_\chi}(t) := \sum_{|k| < S_\chi} \left(1 - \frac{|k|}{S_\chi}\right) c_k(\chi_{n, N, M, L}) e^{ikt}, \quad (21)$$

where S_χ is a positive integer smaller than L .

3.5 Fourier estimators of the derivatives of the leverage

The Continuous Mapping Theorem ensures that the ratio of the non-parametric Fourier estimators (21) and (16), i.e.,

$$\frac{\widehat{\chi}_{n, N, M, L, S_\chi}(t)}{\widehat{v}_{n, N, S_v}(t)} \quad (22)$$

is a consistent estimator of the derivative of the leverage process with respect to the log-price process under (1), as given in (6). Analogously, it also ensures that the ratio of the non-parametric Fourier estimators (21) and (18), i.e.,

$$\frac{\widehat{\chi}_{n, N, M, L, S_\chi}(t)}{\widehat{\eta}_{n, N, M, S_\eta}(t)}, \quad (23)$$

is a consistent estimator of the derivative of the leverage process with respect to the volatility process under (8), as given in (7)⁵.

⁴Note that these conditions also imply that $M^2/n \rightarrow 0$, satisfying the hypotheses of Theorem 2.

⁵For n finite, estimators (22) and (23) are undefined if, respectively, $\widehat{v}_{n, N, S_v}(t)$ or $\widehat{\eta}_{n, N, M, S_\eta}(t)$

4 Simulation study

Given the availability of consistent Fourier estimators of the volatility, the leverage and the derivatives of the leverage with respect to the log-price or the volatility, a simple test to check with empirical data if the true model-free derivatives of the leverage match the corresponding model-dependent predictions under the CEV model, as given in equations (6) and (7), entails performing a linear regression between numerical approximations of the true derivatives, obtained via finite differences, and estimates of the corresponding theoretical derivatives, as given in (22) and (23). Formally, the test involves estimating the linear models

$$\frac{\widehat{\eta}_{n,N,M,S_\eta}(t+h) - \widehat{\eta}_{n,N,M,S_\eta}(t)}{x(t+h) - x(t)} = \alpha_1 \frac{\widehat{\chi}_{n,N,M,L,S_\chi}(t)}{\widehat{v}_{n,N,S_v}(t)} \quad (24)$$

and

$$\frac{\widehat{\eta}_{n,N,M,S_\eta}(t+h) - \widehat{\eta}_{n,N,M,S_\eta}(t)}{\widehat{v}_{n,N,S_v}(t+h) - \widehat{v}_{n,N,S_v}(t)} = \alpha_2 \frac{\widehat{\chi}_{n,N,M,L,S_\chi}(t)}{\widehat{\eta}_{n,N,M,S_\eta}(t)}. \quad (25)$$

If the estimation with empirical data yields statistically-significant estimates of the coefficients α_1 and α_2 that are close to the value of 1, then the predictions of the CEV model could be deemed as an accurate gauge of the true sensitivity of the leverage to changes in the price and the volatility. This in turn would suggest that empirical data support the interpretation of $\chi(t)$ as the process that captures the response of the leverage to changes in the price and the volatility, as implied by the CEV model via equations (6) and (7).

In order to obtain reliable results from the tests (24) and (25), it is not only crucial that finite-sample efficient Fourier-based estimates of the paths of the processes $v(t)$, $\eta(t)$ and $\chi(t)$ are used, but also that the step h for the differentiation procedure is carefully selected. Accordingly, the aim of the simulation study performed in this section is to provide guidance for the optimal selection of the step h .

For the simulation study, we generate price observations from the CEV model in equation (1), setting $\sigma = 0.3$ and $\delta = 0.5$. These parameter values are taken from the simulation study in Sanfelici and Mancino (2020). Further, the initial price value $X(0)$ is selected as $X(0) = 1$. Recall that a value of δ smaller than 1 reproduces the type of leverage effect usually observed on equity markets, that is, it yields a correlation between returns and volatility changes with negative sign.

is equal to zero. However, the analysis conducted in this chapter is not affected by this potential problem, as estimators (22) and (23) are used only in equations (24) and (25), which are rewritten, to reduce numerical instabilities as, respectively, (26) and (27).

Based on these parameter values, we simulate a total of 100 days of 1-second observations. Each simulated day is 6.5-hour long.

Specifically, we simulate two scenarios: one where the efficient log-price $x(t)$ is observable and another, more realistic, where one can only observe the noisy price $\tilde{x}(t) := x(t) + \varepsilon(t)$, that is, the efficient price $x(t)$ contaminated by the presence of an i.i.d. zero-mean microstructure noise component $\varepsilon(t)$. For the simulation of $\varepsilon(t)$, we choose a Gaussian distribution, with standard deviation parameter equal to 10^{-4} .

In both simulated scenarios, we use all available data for the estimation of $v(t)$, $\eta(t)$ and $\chi(t)$, that is, we select $n = 23400$, which corresponds to the 1-second sampling frequency. Further, we make the following selections for the cutting frequencies. At the first level, to obtain spot volatility estimates, we select $N = n/2$ in the noise-free scenario, while in the noisy scenario we select N based on the noise-robust procedure proposed by Mancino and Sanfelici (2008); then, we select $S_v = n^{0.5}$. At the second level, we estimate the spot leverage by choosing $M = n^{0.5}$ and $S_\eta = 4n^{0.25}$. Finally, we select $L = 4n^{0.25}$ and $S_\chi = 6n^{0.125}$ at the third level, to obtain spot estimates of $\chi(t)$. All these selections, with the exception of N , are based on the numerical minimization of the mean-squared error (MSE). The estimated trajectories of $v(t)$, $\eta(t)$ and $\chi(t)$ in the absence and the presence of noise are plotted, along with the corresponding true values, in Figures 1 and 2 to demonstrate the accuracy of the estimation. Additionally, in Figures 1 and 2 we also show the accuracy of the estimated trajectory of $\xi(t)$, which will be used in the final part of the simulation study. Note that the selection of the cutting frequencies for the estimation of $\xi(t)$ is performed separately (see Theorem 3). In particular, first we select N either equal to $3n^{0.75}$ in the noise-free scenario or via the noise-robust approach by Mancino and Sanfelici (2008) in the noisy scenario, then we choose $M = 2n^{0.25}$ and $S_\xi = n^{0.25}$ based on the numerical optimization of the MSE.

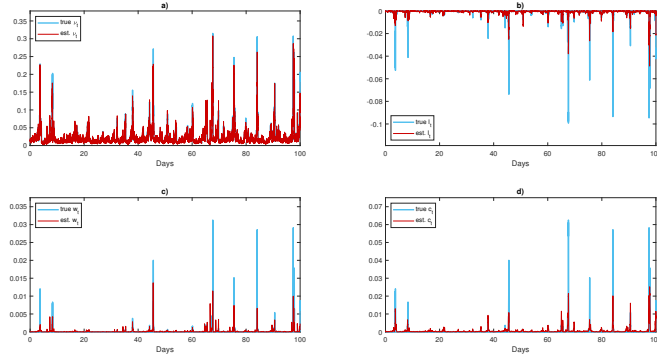


Figure 1: Comparison, in the noise-free scenario, between the true and the estimated trajectories of $v(t)$ (panel a)), $\eta(t)$ (panel b)), $\xi(t)$ (panel c)) and $\chi(t)$ (panel d)). For each panel, the true and estimated trajectories are plotted on the equally-spaced grid of mesh size equal to 1 second.

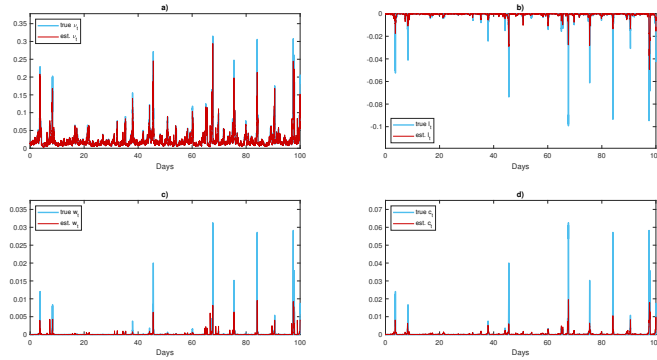


Figure 2: Comparison, in the noisy scenario, between the true and the estimated trajectories of $v(t)$ (panel a)), $\eta(t)$ (panel b)), $\xi(t)$ (panel c)) and $\chi(t)$ (panel d)). For each panel, the true and estimated trajectories are plotted on the equally-spaced grid of mesh size equal to 1 second.

After having obtained accurate estimates of $v(t)$, $\eta(t)$ and $\chi(t)$, we perform tests (24) and (25). In this regard, to reduce the numerical instabilities related to the computation of ratios, we estimate α_1 and α_2 after rewriting (24) and (25) as,

respectively,

$$\left[\widehat{\eta}_{n,N,M,S_\eta}(t+h) - \widehat{\eta}_{n,N,M,S_\eta}(t) \right] \widehat{v}_{n,N,S_v}(t) = \alpha_1 \left[x(t+h) - x(t) \right] \widehat{\chi}_{n,N,M,L,S_\chi}(t), \quad (26)$$

and

$$\left[\widehat{\eta}_{n,N,M,S_\eta}(t+h) - \widehat{\eta}_{n,N,M,S_\eta}(t) \right] \widehat{\eta}_{n,N,M,S_\eta}(t) = \alpha_2 \left[\widehat{v}_{n,N,S_v}(t+h) - \widehat{v}_{n,N,S_v}(t) \right] \widehat{\chi}_{n,N,M,L,S_\chi}(t) \quad (27)$$

The estimates of α_1 and α_2 in the noise-free and the noisy scenarios, obtained for different values of the step h , are plotted in Figures 3 - 6⁶. These figures show that the estimates of α_1 and α_2 fluctuate around the true level, that is, around 1, for values of h between 5 and 30 minutes⁷. This suggests that a more reliable estimate of α_1 or α_2 could be obtained by computing the average of point-wise estimates in correspondence of values of h between 5 and 30 minutes. Indeed, such averages, which are also plotted in Figures 3 - 6 (see the red dashed lines), appear to be very close to 1. The exact averages of the estimates of α_1 and α_2 , along with average values of other relevant outputs of the estimation procedure, are reported in the Table 1. Note that these averages are quite accurate, that is, are quite close to 1. Also, note that point-wise coefficient estimates are all statistically significant, with a constant p-value equal to zero for both tests in both scenarios considered. Finally, note that the very large R^2 values confirm the accuracy of the Fourier estimates of $v(t)$, $\eta(t)$ and $\chi(t)$.

As mentioned in the previous section, based on equations (4) and (11), another aspect that could be investigated empirically is the existence of a linear link between $\chi(t)$ and the vol-of-vol $\xi(t)$. Specifically, the existence of such a link could be investigated by performing the linear regression

$$\widehat{\chi}_{n,N,M,L,S_\chi}(t) = \alpha_3 \widehat{\xi}_{n,N,M,S_\xi}(t). \quad (28)$$

A statistically-significant estimate of the coefficient α_3 would offer evidence, in a model-free setting, that $\chi(t)$ is actually linear in $\xi(t)$, as predicted by the CEV model (and, more generally, by the large class of models represented by (8)). Interpreting $\chi(t)$ as the process that captures the response of the leverage to changes in the volatility or the price, this would mean that the latter is proportional to the

⁶Note that the estimation of α_1 and α_2 has been performed using the robust regression method with a bisquare weighting scheme to penalize outliers (see Holland and Welsch (1977)). The same holds for the estimation of α_1 and α_2 in the empirical study of the next section.

⁷For h smaller than 5 minutes, estimates of α_1 and α_2 tend to be biased and very noisy and thus are omitted from the plots.

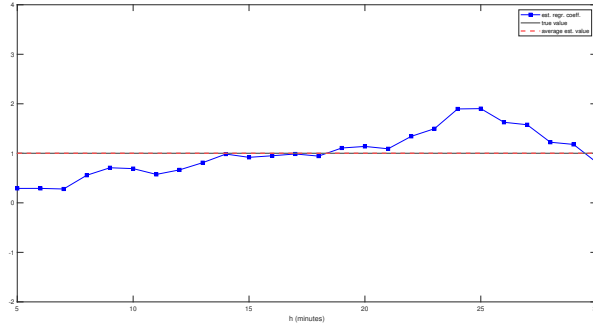


Figure 3: Estimation of model (24) in the noise-free scenario: comparison of point-wise estimates of the coefficient α_1 in correspondence of different values of the step h (in blue) and their average (red dashed line) with the true value (grey line).

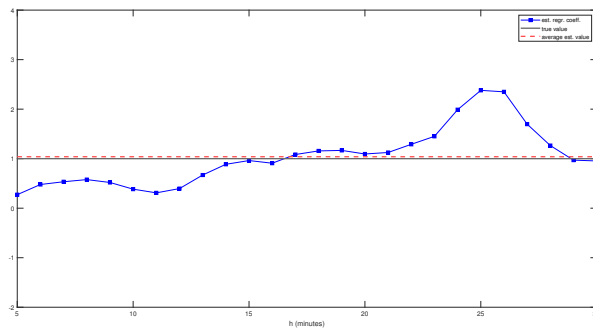


Figure 4: Estimation of model (24) in the noisy scenario: comparison of point-wise estimates of the coefficient α_1 in correspondence of different values of the step h (in blue) and their average (red dashed line) with the true value (grey line).

uncertainty perceived by market operators about the actual riskiness of the asset of interest (i.e., the vol-of-vol $\xi(t)$).

As for (24) and (25), the accuracy of the regression (28) can also be tested on simulated observations from the CEV model, to obtain guidance for the selection of the optimal frequency for the sampling of Fourier estimates of $\chi(t)$ and $\xi(t)$. Estimates of α_3 in correspondence of different sampling frequencies between 5 and 30 minutes are shown in Figures 7 and 8. Note that point-wise estimates of α_3

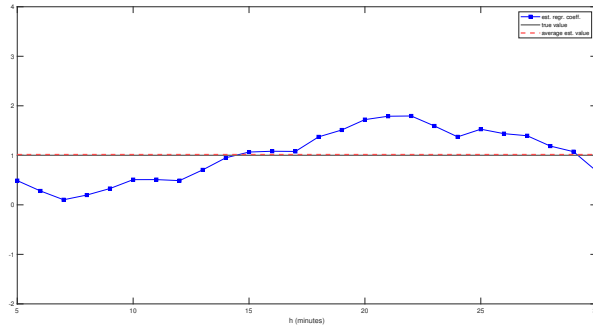


Figure 5: Estimation of model (25) in the noise-free scenario: comparison of point-wise estimates of the coefficient α_2 in correspondence of different values of the step h (in blue) and their average (red dashed line) with the true value (grey line).

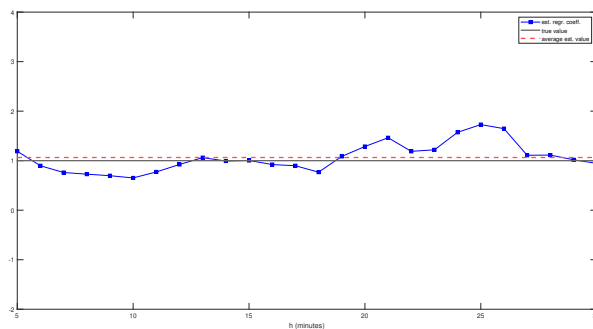


Figure 6: Estimation of model (25) in the noisy scenario: comparison of point-wise estimates of the coefficient α_2 in correspondence of different values of the step h (in blue) and their average (red dashed line) with the true value (grey line).

appear to be very reliable, in that they are all very close to the true value of 2, at least for sampling frequencies smaller than 15 minutes. However, a conservative approach might suggest to adopt the average as a final estimate of α_3 also in this case (see the red dashed line in Figures 7 and 8). Average statistics of the regression are reported in Table 2⁸. Again, we obtain quite satisfactory R^2 values, which

⁸To account for auto-correlations in the residuals, we compute Newey-West standard errors, see Newey and West (1987). We do the same also when estimating α_3 in the empirical exercise of the

	coeff. est.	std. err.	t stat.	p-value	R^2
model (24), w/o noise	1.001 (0.550)	0.004 (0.001)	240.538 (110.971)	0 (0)	0.906 (0.138)
model (24), w/ noise	1.039 (0.654)	0.005 (0.002)	188.964 (81.688)	0 (0)	0.877 (0.190)
model (25), w/o noise	1.016 (0.587)	0.002 ($< 10^{-3}$)	590.663 (290.443)	0 (0)	0.955 (0.120)
model (25), w/ noise	1.064 (0.395)	0.002 ($< 10^{-3}$)	636.648 (223.603)	0 (0)	0.992 (0.005)

Table 1: Estimation results for models (24) and (25): average values of coefficient estimates, standard errors, t statistics, p-values and R^2 , computed for h ranging between 5 and 30 minutes. Standard deviations are also reported in brackets. For each model, the lines “w/o noise” and “w/ noise” refer to, respectively, the simulated scenario without and with noise.

confirm the accuracy of the estimates of $\chi(t)$ and $\xi(t)$; also, all estimates of α_3 are significant, with constant p-values equal to zero.

Finally, note that we obtain comparable results in the noise-free and noisy scenarios for all three tests performed in this section, thereby confirming the robustness of the Fourier methodology to the presence of noise.

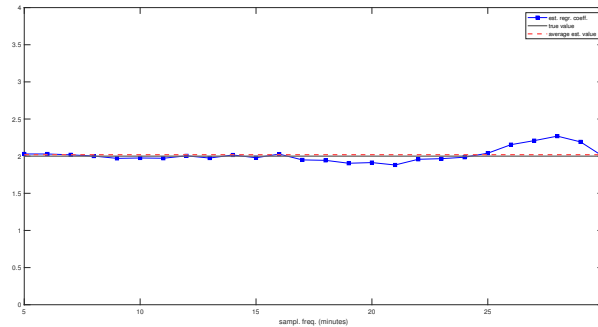


Figure 7: Estimation of model (28) in the noise-free scenario: comparison of point-wise estimates of the coefficient α_3 in correspondence of different sampling frequencies (in blue) and their average (red dashed line) with the true value (grey line).

next section.

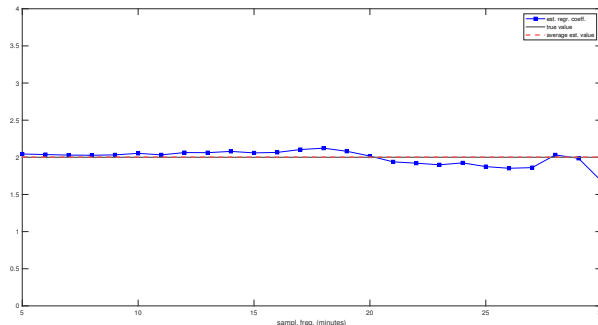


Figure 8: Estimation of model (28) in the noisy scenario: comparison of point-wise estimates of the coefficient α_3 in correspondence of different sampling frequencies (in blue) and their average (red dashed line) with the true value (grey line).

	coeff. est.	std. err.	t stat.	p-value	R^2
model (28), w/o noise	2.003 (0.126)	0.326 (0.045)	6.280 (1.177)	0 (0)	0.543 (0.032)
model (28), w/ noise	2.020 (0.157)	0.233 (0.041)	8.918 (1.671)	0 (0)	0.538 (0.038)

Table 2: Estimation results for models (24) and (25): average values of coefficient estimates, standard errors, t statistics, p-values and R^2 , computed for sampling frequencies ranging between 5 and 30 minutes. Standard deviations are also reported in brackets. The lines “w/o noise” and “w/ noise” refer to, respectively, the simulated scenario without and with noise.

5 Empirical study

In this section we perform tests (24), (25) and (28) on the series of 1-second S&P500 price observations over the period March, 2018 – April, 2018 (see Figure 9).

To obtain Fourier estimates of the paths of $\nu(t)$, $\eta(t)$, $\chi(t)$ and $\xi(t)$, we use all data in the sample, that is, we select $n = 23400$, corresponding to the 1-second sampling frequency. Further, we select the cutting frequencies using as guidance the MSE-optimal values obtained via simulations in the noisy scenario of Section 4. Specifically, after choosing N via the noise-robust procedure given in Mancino and Sanfelici (2008), we select $S_\nu = M = n^{0.5}$, $S_\eta = L = 4n^{0.25}$ and $S_\chi = 6n^{0.125}$. For the estimation of $\xi(t)$, instead, we select $M = 2n^{0.25}$ and $S_\xi = n^{0.25}$. The

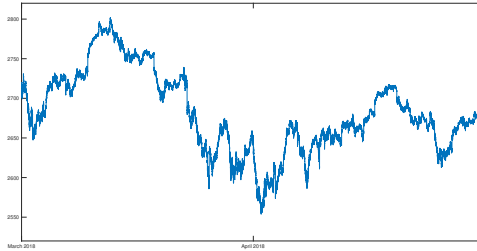


Figure 9: S&P 500 1-second prices over the period March, 2018 – April, 2018.

estimated trajectories of $v(t)$, $\eta(t)$, $\xi(t)$ and $\chi(t)$ are plotted in Figure 10. Note that, before performing the estimation, we have removed days with price jumps from the 2-month sample, using the jump detection test by Corsi et al. (2010). In particular, the test at 99.9% confidence level detects only two days with jumps, namely March 20th and March 23rd. These two days are associated with market turbulence related to the so-called “trade war” between China and the US.

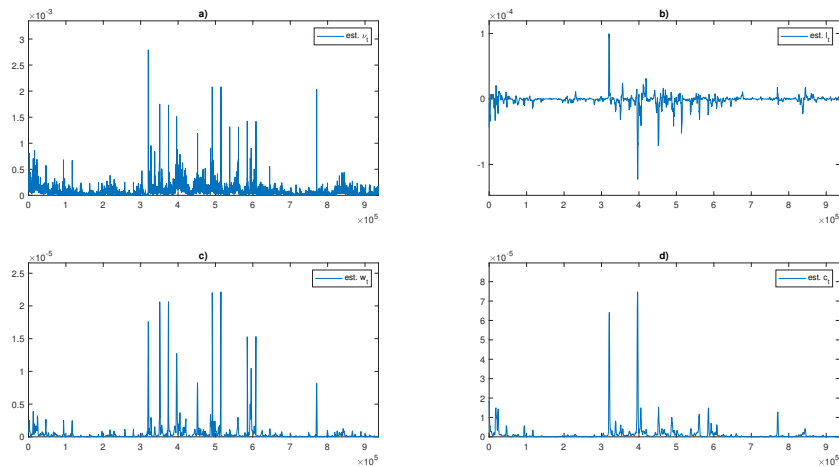


Figure 10: Reconstructed 1-second trajectories of $v(t)$, $\eta(t)$, $\xi(t)$ and $\chi(t)$ for the S&P 500 index over the period March, 2018-April, 2018.

Using the reconstructed paths of $v(t)$, $\eta(t)$, $\chi(t)$ and $\xi(t)$ we then perform tests

(24), (25) and (28)⁹. The results are summarized in Table 3 and Figures 11 - 13.

Overall, the results of tests (24) and (25) support the interpretation of the process $\chi(t)$ as a process that captures the instantaneous response of the leverage to changes in the price and the level of market risk (i.e., the volatility). In fact, not only we obtain statistically-significant estimates of α_1 and α_2 for all values of h considered, but also these estimates fluctuate around average estimates which are close to 1, taking values equal, respectively, to 1.018 and 0.914

Additionally, the results of test (28) support the existence of a statistically-significant positive linear dependence between $\chi(t)$ and $\xi(t)$. This empirical result, if considered jointly with the results of tests (24) and (25), suggests that the sensitivity of the leverage to changes of the price or the volatility is larger when the uncertainty about the actual level of risk perceived on the market (i.e., the vol-of-vol) is larger. Additionally, note that point-wise estimates of α_3 are close to 2, the value predicted by the CEV model, with a final average estimate equal to 1.895.

Finally, note that we obtain R^2 values which are not far from the values obtained in simulations, for all three tests. This suggests that the tested models fit the sample data quite well.

	coeff. est.	std. err.	t stat.	p-value	R^2
model (24)	1.018 (1.119)	0.006 (0.004)	163.605 (159.688)	0 (0)	0.821 (0.225)
model (25)	0.914 (0.660)	0.009 (0.002)	92.858 (73.879)	0 (0)	0.847 (0.159)
model (28)	1.895 (0.206)	0.625 (0.049)	3.037 (0.323)	0.004 (0.003)	0.409 (0.038)

Table 3: Estimation results for models (24), (25) and (28): average values of coefficient estimates, standard errors, t statistics, p-values and R^2 , computed for values of h (models (24) and (25)) or sampling frequencies (model (28)) ranging between 5 and 30 minutes. Standard deviations are also reported in brackets.

6 Conclusions

The main finding of this paper is uncovering, both from an analytical and an empirical perspective, the relationship between the price-leverage covariation and the sensitivity of the leverage process to changes in the price or the volatility.

⁹To avoid performing a spurious regression (see Granger and Newbold (1974)), we test for the null hypothesis of the presence of a unit root in the all the series of regressors and regressands involved, using the Augmented Dickey-Fuller test (see Dickey and Fuller (1979)). For all series, test results at the 99.9% confidence level reject the null hypothesis.

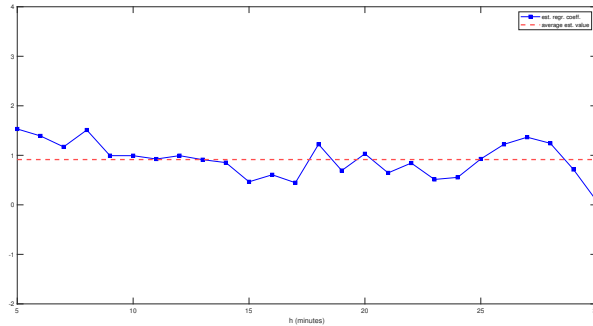


Figure 11: Estimation of model (24): point-wise estimates of the coefficient α_1 in correspondence of different sampling frequencies (in blue), along with their average (red dashed line).

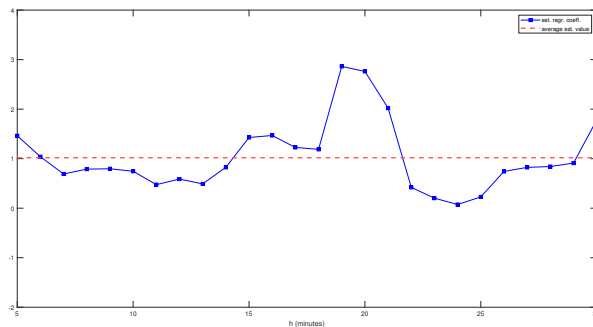


Figure 12: Estimation of model (25): point-wise estimates of the coefficient α_2 in correspondence of different sampling frequencies (in blue), along with their average (red dashed line).

Indeed, first we show that under the CEV model, which is explicitly designed to capture the leverage effect, the derivatives of the leverage process with respect to the price and the volatility are equal to the price-leverage covariation scaled, respectively, by the volatility and the leverage itself. In this regard, we stress that a key analytical result we obtain is expressing the derivatives of a stochastic process (the leverage) as a function of objects that can be consistently estimated from sample prices over a fixed time horizon, that is, iterated covariances.

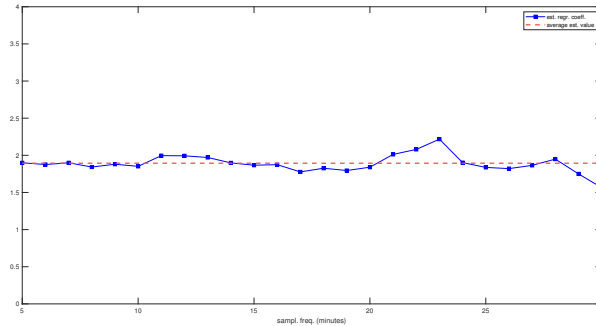


Figure 13: Estimation of model (28): point-wise estimates of the coefficient α_3 in correspondence of different sampling frequencies (in blue), along with their average (red dashed line).

Then, after reconstructing the paths of the volatility, the leverage and the price-leverage covariation by means of the (non-parametric) Fourier methodology, we show, empirically, that these model-dependent predictions reproduce the model-free derivatives of the leverage quite accurately in the case of the S&P500 index over the period March, 2018-April, 2018.

Based on this empirical evidence, the price-leverage covariation could be understood by market operators as a gauge of the responsiveness of the leverage effect to the arrival of new information causing a change in the price level and/or the amount of market risk, that is, in the volatility.

Additionally, based on the existence of a linear link between the price-leverage covariation and the vol-of-vol under the CEV model, we also investigate the empirical dependence between these two quantities in model-free setting, that is, using non-parametric Fourier estimates of their paths. In this regard, empirical results support the existence of a statistically significant linear link, with a coefficient close to 2, the value predicted by the CEV model. This in turn suggests that the response of the leverage is stronger when the uncertainty about the actual level of risk perceived, i.e., the vol-of-vol, is larger (and viceversa).

References

Aït-Sahalia, Y. and Jacod, J. (2014). High-frequency financial econometrics. *Princeton University Press*.

- Araneda, A. (2020). The fractional and mixed-fractional cev model. *Journal of Computational and Applied Mathematics*, 363(1):106–123.
- Bandi, F. and Renò, R. (2012). Time-varying leverage effects. *Journal of Econometrics*, 169(1):94–113.
- Barucci, E., Malliavin, P., Mancino, M. E., Renó, R., and Thalmaier, A. (2003). The price volatility feedback rate: an implementable mathematical indicator of market stability. *Mathematical Finance*, 13(1):17–35.
- Barucci, E. and Mancino, M. E. (2010). Computation of volatility in stochastic volatility models with high-frequency data. *International Journal of Theoretical and Applied Finance*, 13(5):767–787.
- Beckers, S. (1980). The constant elasticity of variance model and its implications for option pricing. *The Journal of Finance*, 35(3):661–673.
- Chan, K. C., Karolyi, G. A., Longstaff, F. A., and Sanders, A. B. (1992). An empirical comparison of alternative models of the short-term interest rate. *The Journal of Finance*, 47(3):1209–1227.
- Corsi, F., Pirino, D., and Renò, R. (2010). Threshold bipower variation and the impact of jumps on volatility forecasting. *Journal of Econometrics*, 159(2):276–288.
- Derman, E. and Kani, I. (1994). Riding on the smile. *RISK*, 7:32–39.
- Dickey, D. A. and Fuller, W. A. (1979). Distribution of the estimators for autoregressive time series with a unit root. *Journal of the American Statistical Association*, 74(366):427–443.
- Dupire, B. (1994). Pricing with a smile. *RISK*, 7:18–20.
- Feller, W. (1951). Two singular diffusion problems. *Annals of Mathematics*, 54(1):173–182.
- Granger, C. W. J. and Newbold, P. (1974). Spurious regressions in econometrics. *Journal of Econometrics*, 2(2):111–120.
- Heston, S. (1993). A closed-form solution for options with stochastic volatility with applications to bond and currency options. *The Review of Financial Studies*, 6(2):327–343.
- Hobson, D. and Rogers, L. (1998). Complete models with stochastic volatility. *Mathematical Finance*, 8:27–48.

- Holland, W. P. and Welsch, R. E. (1977). Robust regression using iteratively reweighted least-squares. *Communications in Statistics - Theory and Methods*, 6(9):813–827.
- Kalnina, I. and Xiu, D. (2017). Nonparametric estimation of the leverage effect: a trade-off between robustness and efficiency. *Journal of the American Statistical Association*, 112(517):384–399.
- Malliavin, P. and Mancino, M. E. (2002). Fourier series method for measurement of multivariate volatilities. *Finance and Stochastics*, 6(1):49–61.
- Malliavin, P. and Mancino, M. E. (2009). A fourier transform method for nonparametric estimation of multivariate volatility. *The Annals of Statistics*, 37(4):1983–2010.
- Mancino, M. E., Recchioni, M. C., and Sanfelici, S. (2017). Fourier-malliavin volatility estimation: Theory and practice. *Springer*.
- Mancino, M. E. and Sanfelici, S. (2008). Robustness of fourier estimator of integrated volatility in the presence of microstructure noise. *Computational Statistics and Data Analysis*, 52(6):2966–2989.
- Nelson, D. B. (1990). Arch models as diffusion approximations. *Journal of Econometrics*, 45(2):7–38.
- Newey, W. K. and West, K. D. (1987). A simple, positive semi-definite, heteroskedasticity and autocorrelation consistent covariance matrix. *Econometrica*, 55(3):703–708.
- Platen, E. (1997). A non-linear stochastic volatility model. *Financial Mathematics Research Report No.FMRR005-97, Center for Financial Mathematics, Australian National University*.
- Sanfelici, S., Curato, I. V., and Mancino, M. E. (2015). High frequency volatility of volatility estimation free from spot volatility estimates. *Quantitative Finance*, 15(8):1331–1345.
- Sanfelici, S. and Mancino, M. E. (2020). Identifying financial instability conditions using high frequency data. *Journal of Economic Interaction and Coordination*, 15:221–242.